WITHDRAWN: Decellularized Lung Extracellular Matrix Scaffold Promotes Human Embryonic Stem Cell Differentiation Towards Alveolar Progenitors

Afshin Noori
University of Tehran
Mohammad Reza Mokhber Dezfouli
University of Tehran
Sarah Rajabi
Royan Institute
Fatemeh Ganji
Iran University of Medical Sciences
Zahra Ghezelayagh
Royan Institute
Elie El Agha
Universities of Giessen and Marburg Lung Center
Hossein Baharvand
Royan Institute
Sirous Sadeghian Chaleshtori
University of Tehran
Yaser Tahamtani
yasertahamtani@gmail.com

Royan Institute

Research Article

Keywords: Decellularized lung, ECM, Hydrogel, PSCs, lung progenitors, alveolar cells

Posted Date: June 21st, 2021

DOI: https://doi.org/10.21203/rs.3.rs-618083/v1

Additional Declarations: No competing interests reported.

EDITORIAL NOTE:

The full text of this preprint has been withdrawn by the authors while they make corrections to the work. Therefore, the authors do not wish this work to be cited as a reference. Questions should be directed to the corresponding author.

Abstract

Efficient production of alveolar epithelial cells and achieving optimal functionality and maturity has presented a serious challenge in recent years. The extracellular matrix (ECM) provides a dynamic environment and mediates cellular responses during both development and tissue repair. Decellularized ECM (dECM) which retains its native-like structure and biochemical composition provides the signals needed to induce differentiation into tissue-specific lineages *in vitro.* Here, we repopulated lung ECM-derived scaffold (scaffold) with human embryonic stem cells (hESCs) derived lung progenitor cells and compared with the cells grown on either lung ECM-derived hydrogel (hydrogel) or fibronectin-coated plates in 2D cultures. We found that scaffold preserved its composition and native structures. All groups displayed progenitor cell differentiation as revealed by the expression of *NKX2.1*, *P63,* and *CK5*. Although no significant differences in cell viability between groups, cells differentiated on scaffold and hydrogel showed significant upregulation of *SOX9* (a marker of the distal airway epithelium), cells differentiated on scaffold showed enhanced expression of *SFTPC* (AT2 marker), *FOXJ1* (ciliated cell marker) and *MUC5A* (secretory cell marker). Overall, our results suggest that scaffold improves differentiation of progenitors into alveolar type 2 cells in comparison with hydrogel and fibronectin as well as efficient retention and homing to the alveolar region.

1. Introduction

The native lung ECM contains major biochemical and biophysical cues that provide biocompatibility, elasticity and porosity requirements supporting cell attachment and fate decision making. Therefore, it is ideal for lung tissue engineering and likely represents a better strategy than artificial matrices designed to mimic lung ECM [1,2]. In addition to biochemical cues, physical interaction between cells and the underlying ECM mediates stem cell behavior such as proliferation, migration and differentiation [3,4].

Pluripotent stem cell (PSC)-derived cells are potentially influenced by ECM and exogenous signals such as paracrine-acting growth factors, and instructive memory in native ECM is able to developmentally determine cell fate and promote tissue-specific differentiation [5]. In this regard, decellularized ECM has been generated from various organs, used as scaffold and recellularized with various cells to study cell-ECM interactions for organ engineering [5–7]. Therefore, decellularized lung scaffolds have been repopulated with primary cells or cells in predifferentiation states derived from PSCs to demonstrate the efficient generation of mature airway structures in vitro [8,9].

Previous reports demonstrated type 2 alveolar epithelial cell (AT2)-like progenitor cell differentiation from PSCs using stepwise differentiation protocols that are initiated by definitive endoderm (DE) differentiation [10–12]. PSCs are able to efficiently generate DE after exposure to activin A and, in other modified methods, combined with small molecule CHIR99021 (GSK3 inhibitor/WNT activator agonist) for 3 or 5 4 days. In the next step, inhibition of TGF/BMP and Wnt signaling in PSC-derived DE provides a signal for anterior foregut endoderm (AFE) generation. AFE cells are specified toward early lung

progenitors (NKX2-1$^+$ cells) with multipotent capabilities .Subsequently, the cells are exposed to the WNT agonist, FGF10 and KGF leading to surfactant proteins expressing cells differentiation [9].

The ability to generate AT2 cells has been explored and current protocols yielded most cell types of the respiratory system which have been reviewed above. Additionally, PSC-derived lung progenitors are capable to repopulate human and rat decellularized lung matrices and differentiate distal lung cell types. So, an animal source for xeno-organs as scaffolds for human tissues may resolve the lung donor shortage and facilitate lung tissue engineering process. Also, highly conserved of ECM components led researchers to include xenogeneic scaffolds which have already been utilized in clinical practice, including heart valve replacement and wound care [13–15].

In Iran, sheep lung tissues are a by-product of the food industry, so we could easily obtain donor tissues for our experiments. Here, we aimed to elucidate whether sheep lung ECM-derived scaffold provides crucial cues for the differentiation and further maturation of ESC-derived progenitor cells. We generated sheep decellularized lung ECM and then seeded human ESC-derived progenitor cells under defined conditions to investigate the potential of scaffold in promoting alveolar epithelial cell differentiation. We compared the efficacy of recellularized scaffold method with differentiation on fibronectin- or lung ECM-derived hydrogel-coated plates. We show that seeding cells on scaffold highly upregulates early lung progenitor cell genes as well as genes that are characteristic of proximal airway epithelial cells and AT2.

2. Materials And Methods

2.1. Lung decellularization

To ensure a sufficient supply of lung ECM needed for the experiments and to minimize potential variation in matrix compounds between samples, one sheep lung which is a by-product tissue in the food industry in Iran was used. Animal experiment were approved by Institutional Animal Care and Use Committee (approval code: IR.ACECR.ROYAN.REC.1397.271). All experimental protocols were approved by a Royan Institute. Fresh lung tissues (the superior and inferior cranial lobe pieces of sheep lung with intact small airways and vessels) were promptly delivered to the laboratory and cut into 5×5×1 mm pieces under sterile conditions. Lung pieces were rinsed with distilled water several times for 30 min to remove blood cells and decellularization was then achieved by 1% sodium deoxycholate (SDC, Sigma) at 4°C for 24 h. Lung pieces were then soaked in 1 M NaCl (Sigma) solution for 1 h. After the decellularization process, the acellular lung matrix was rinsed with double-distilled water for 48 h. Finally, samples were soaked in 70% ethanol for a 10 s under sterile conditions. To remove ethanol, samples were washed with phosphate buffer saline (PBS, Gibco) several times over a period of 3 days. The procured lung matrices were stored at 4°C for short-term use and at -20°C for long-term storage. All methods were carried out in accordance with the ARRIVE guidelines. All methods were carried out in accordance with relevant guidelines and regulations.

2.2. Characterization of decellularized lung tissues

2.2.1. Histological evaluation

Acellular lung pieces (n = 5) were randomly selected and fixed in formalin for 4 h. The fixed acellular lung matrix was incorporated in agar gel (2%) followed by tissue processing. Samples were then paraffin-embedded and sectioned into 6 μm-slices. After deparaffinization, slices were stained with hematoxylin and eosin (H&E) to confirm the absence of nuclei. Additionally, staining with 4,6-diamidino-2-phenylindole (DAPI, Sigma-Aldrich) was carried out. The acellular lung matrix was evaluated for collagen and glycosaminoglycan content by Masson's trichrome (MT) and Alcian Blue (AB) staining, respectively. Specimens were finally analyzed by light microscopy (BX51, Olympus) and imaged with an Olympus DP72 digital camera that was mounted on the microscope.

2.2.2. DNA content

To assess and quantify total DNA content, 30 mg of lyophilized native and decellularized lung tissues were treated with digesting buffer solution containing 50 mM Tris-HCl (pH 8), 50 mM EDTA, 10 mM NaCl and 1% SDS in the presence of proteinase K overnight at 65°C. Supernatants were purified using phenol-chloroform (500 μl to each sample) followed by centrifugation. The upper layer was collected and centrifuged. The aqueous layer was then removed, subjected to ethanol precipitation and dried. After suspension in diH2O, absorbance was measured at 260 nm using a spectrophotometer.

2.2.3. Evaluating the ultrastructure of decellularized lung ECM (dECM)

Decellularized lung pieces (2 g) were lyophilized using CHRIST lyophilizer (Alpha 1–2 LD plus, Germany) and gold-coated using an Emitech K575X Sputter coater. Electron micrographs were captured at a 100x magnification with a scanning electron microscope (VEGA, TESCAN, Czech Republic).

2.3. Hydrogel preparation and coating

Decellularized lung pieces were lyophilized and milled to prepare lung powder. The powder was then digested with pepsin at a concentration of 1 mg/mL in 0.1 M HCl and stirred at 4°C for 60 h. Afterwards, the solution was neutralized with 1 M NaOH at 4°C to induce gelation. After sterilization by UV irradiation, a working concertation of gel solution was prepared by diluting in Dulbecco's modified Eagle's medium (DMEM). Then, followed by incubation at 37°C for 5 min. To determine the proper concentration of gel solution for cell culture application, four concentrations of gel solution (1, 2, 3 and 5 mg/mL) were tested, and their impact on cell growth was analyzed by assessing A549 cell line confluency after 6 days.

2.4. Fibronectin coating

Plates were positively charged with 50 μg/mL of poly-L-ornithine (PLO) to enhance cell attachment and were then incubated at 37°C for 1 h. After PLO removal, plates were rinsed 3 times with PBS followed by fibronectin (Sigma-Aldrich) coating at a concentration of 50 μg/mL. Finally, plates were incubated at 37°C for 24 h and stored at 4°C for further experiments.

2.5. Proliferation assay

To examine the efficacy of different coating conditions and analyze their impact on cell proliferation, A549 cells were prepared in the desired concentration (5000 cells per well) and seeded on three different beds: (1) fibronectin-coated plates; (2) lung ECM-derived hydrogel (Gel); and (3) decellularized lung pieces (dECM). At day 7, 20 µL of MTS reagent (Promega) was added into each well containing 100 µL of culture medium followed by incubation at 37°C for 4 h in a humidified chamber with 5% CO_2. Absorbance was recorded at a wavelength of 490 nm.

2.6. Human embryonic stem cell (hESC) culture and differentiation

hESC line RH5 (24), obtained from the Royan Stem Cells Bank (Royan Institute), was cultured on mouse embryonic fibroblasts (MEFs) as a feeder-containing condition. To initiate differentiation, feeder-containing hESC cultures were switched to feeder-free system; hESCs were cultured in 6-well Matrigel-(Sigma-Aldrich) coated plates in DMEM/F12 (Life Technologies) supplemented with 20% knockout serum replacement (Life Technologies), 2 mM l-glutamine (Gibco), 0.1 mM non-essential amino acids (NEAAs, Gibco), 1% insulin-transferrin-selenium (ITS, Gibco), 1% penicillin/streptomycin (Gibco), 0.1 mM β-mercaptoethanol (Sigma-Aldrich) and 100 ng/ml basic fibroblast growth factor (bFGF, Royan Biotech). The medium was changed every other day. For maintenance, cells were passaged every 6–8 days on Matrigel. All hESC culture procedures were performed under standard culture conditions of 37°C and 5% CO_2 with approximately 95% relative humidity.

2.6.1. Differentiation of hESCs towards endoderm

At day 4 of hESC culture, the culture medium was changed to endoderm medium consisting of RPMI 1640 (Life Technologies), 1% penicillin/streptomycin, 1% B-27 without vitamin A (Life Technologies) and 0.1% bovine serum albumin (BSA; Life Technologies). To achieve mesoendoderm, 100 ng/ml activin A (Sigma-Aldrich) and 3 µM CHIR99021 (GSK3 inhibitor/Stemgent) were added to the basal medium. After 24 h, CHIR99021 was removed and the cells were treated with 100 ng/ml activin A for 3 days in order to yield the definitive endoderm (Sigma-Aldrich, A4941).

2.6.2. Differentiation of endoderm towards anterior foregut endoderm

On day 4 of endoderm differentiation, colonies were dissociated into single cells using trypsin/EDTA (Gibco). Afterwards, endodermal cells were plated on 3 different beds: (1) 6-well fibronectin-coated plate; (2) 6-well hydrogel-coated plate (lung ECM-derived hydrogel); and (3) lung ECM-derived scaffold (scaffold/24 well plate) (~ 50,000–75,000 cells/cm). DMEM/F12 (1:3) containing 1.5 µM Dorsomorphin (Tocris, R&D Systems) and 10 µM SB431542 (Tocris, R&D Systems) was added for 24 h and then switched to 24 h of 10 µM SB431542 (inhibitor of TGF-beta type I receptor, Sigma) and 1 µM IWP2 (Tocris, R&D Systems).

2.6.3. Induction of lung progenitors

For lung progenitor induction, the achieved AFE was treated with a ventralization cocktail containing 3 μM CHIR99021, 10 ng/mL recombinant human (rh) FGF10, 10 ng/mL rhFGF7, 10 ng/mL rhBMP4, 20 ng/mL recombinant murine (rm)EGF and 0–1 μM all-trans retinoic acid (ATRA) (all from R&D, except CHIR99021 from Stemgent and ATRA from tocris) in differentiation medium for the next 9 days.

On day 15, lung-field progenitor cells were dissociated with 0.05% warm trypsin/ EDTA for 1 min and rinsed with IMDM supplemented with 5% FCS. Then, cells were plated and cultured under the same condition as before (fibronectin, hydrogel and scaffold) at a 1:5 dilution in serum-free conditioned medium containing 3 μM CHIR99021, 10 ng/mL rhFGF10, and 10 ng/mL rhFGF7 for 10 days.

2.7. Evaluation of hPSC-derived lung progenitors cultured on dECM and Gel

2.7.1. Histological preparation

Histological assessment (as described in Sect. 2.2.1) was carried out for differentiated lung progenitors on different beds and analyzed by H&E staining and immunostaining assays.

2.7.2. Immunofluorescence and immunohistochemistry staining

Slides were rehydrated and antigen retrieval was performed using citrate buffer (pH 6.0, Dako, Santa Clara, CA) for 20 min at 120°C. After 1 h of permeabilization and blocking in 0.1% Triton X-100% and 10% secondary antibody host serum with 0.5% bovine serum albumin (BSA, sigma), tissue sections were incubated with primary antibodies against OCT4 (1: 200; Santa Cruz, sc-31984), SOX17 (1: 200; Santa Cruz, sc-130295), FOXA2 (1: 100; Sigma, AB4125), NKX2.1 (1: 100; Abcam, ab227652), P63 (1: 100; Abcam, ab110038), pro-SFTPC (1: 500 ; Abcam, ab40879) overnight at 4°C. Sections were then washed three times with PBS, followed by 1 h of incubation at 37°C with mouse anti-goat FITC (1:400; Santa Cruz), goat anti-mouse FITC (1:400; Invitrogen, A11005) and goat anti-rabbit IgG-TR (1:200; Invitrogen, A11037) secondary antibodies. Nuclei were stained with DAPI (Sigma, Germany) for 2 min. For immunohistochemistry, slides were subjected to antigen retrieval and were then immersed in a 0.1% H_2O_2 solution and blocking with 10% goat serum in PBS at 37°C for 1 h. Afterwards, samples were incubated at 4°C overnight with primary antibodies against AQP3 (1:250), CK5 (1:200), P63 (1:200) and pro-SFTPC (1:400) (all from Abcam). On the following day, samples were stained with HRP-conjugated secondary antibody (1:1000; Sigma-Aldrich) followed by DAB staining. All samples were counterstained with hematoxylin. Finally, sections were mounted and imaged using Olympus BX51 microscope.

2.7.3. Flow cytometry

Differentiated spheres were dissociated into single cells using trypsin/EDTA (Gibco), washed, and collected by centrifugation. Subsequently, dispersed cells were fixed in 4% paraformaldehyde at 4°C for

20 min, permeabilized, and blocked. Next, cells were incubated overnight with anti-SOX17 (1:200; Abcam, ab155402) and anti-FOXA2 (1:100; Sigma, c3062) antibodies for 1–2 h at 4°C. Flow cytometric analysis was performed using BD FACSCalibur sorter (BD Biosciences), and results were analyzed by Flowing Software (version 2.4.2). Flow cytometry for both differentiation protocols was repeated three times in independent experiments.

2.8. Gene expression analysis

Total RNA was extracted using TRIzol (Sigma), and after removal of genomic DNA with DNaseI, 1 µg of total RNA was reverse-transcribed using a RevertAid™ H Minus First Strand cDNA Synthesis Kit (Thermo Fisher Scientific) based on the manufacturer's instructions. Real-time PCR was performed as previously described [16] using StepOnePlus (ABI, USA) and SYBR Green real-time PCR Master Mix (Amplicon). Sample Ct-values were normalized to *GAPDH* as a reference gene (Forward: 5' CTC ATT TCC TGG TAT GAC AC GA 3'/ Reverse: 5' CTT CCT CTT GTG CTC TTG CT 3'). The fold changes were shown relative to the control group (pluripotent stem cells). Relative gene expression levels were calculated after a standard-curve analysis and using the comparative delta-Ct method. Samples were obtained from three independent biological replicates, and all reactions were performed in duplicates. The sequences of primers are listed in supplementary table S1.

2.9. Statistical analysis

Statistical analysis was performed using GraphPad Prism (Version 6.1, GraphPad software, CA, USA). Significant difference was determined by the t-test and data are presented as mean ± standard deviation (SD). Mean differences were considered statistically significant if $p < 0.05$.

3. Results

3.1. Decellularized lung scaffold/ hydrogel characterized for 3D and 2D cell cultures

The process of generating sheep lung hydrogels is depicted in Fig. 1A. Initially, lung pieces were subjected to a chemical procedure to prepare the hydrogel. SDC was used to prepare decellularized lung pieces. After the lyophilization step, lung powder was enzymatically digested to prepare hydrogel. Histological evaluation using H&E and DAPI stainings revealed the overall structure and absence of nuclei in decellularized pieces (Fig. 1B). The collagen and glycosaminoglycan contents were shown to be preserved in these lung scaffold using Alcian blue (glycosaminoglycan), Masson's trichrome (collagen) and Toluidine blue (glycosaminoglycan) stainings (Fig. 1B). SEM photomicrographs confirmed the preservation of porous structures and the absence of intact cells (Fig. 1C). Analysis of preserved glycosaminoglycan content did not show difference between native ECM and decellularized ECM (dECM) (Fig. 1D). DNA content analysis showed a significant decrease in decellularized lung pieces (0.6 ± 0.1 ng/mg) compared with native lung tissue (21.66 ± 2.3 ng/mg) (Fig. 1E).

3.2. High expression of DE specific markers in PSCs after 4 days of induction

Several published studies reported a stepwise method to differentiation DE, AFE, and lung progenitor cells from PSCs [9,17]. In the present study, lung-derived hydrogels and intact ECM were used to improve the phenotype of differentiated lung epithelial cells. Before AFE induction, endodermal cells were plated on 3 different conditions including fibronectin-coated plates, hydrogel-coated plates, and lung ECM-derived scaffold (Fig. 2A). To optimize the condition for further cell culturing experiments, the proliferation of A549 cells on three different beds was assessed by MTS assay on days 1, 3, 7 of culture. The percentage of live cells in the three groups showed no significant differences at days 3 and 7 (Fig. 2B). Cell counting analysis showed that cells grown on hydrogel at a concentration of 1 and 2 mg/mL revealed a significant increase in cell attachment, growth and proper morphology (Fig. S1).

hESCs formed typical colonies with defined borders before differentiation into endoderm, and DE cells appeared in culture after 4 day of endoderm induction (Fig. 2C). During the endodermal differentiation process, two markers of pluripotency (*NANOG* and *OCT4*) showed significant downregulation (Fig. 2D) while DE-specific markers such as *SOX17* and *FOXA2* were significantly upregulated in PSC-derived endodermal cells ($P < 0.05$) (Fig. 2E). Increased expression of SOX17 and FOXA2 was confirmed by immunostaining of endodermal cells at day 4 (Fig. 2F). Flow cytometric findings indicated that 77% of cells were positive for SOX17, 95% for FOXA2 and 77% for both (Fig. 2G).

3.3. Decellularized lung scaffolds or hydrogel coating induce further differentiation of DE cells

To assess the impact of decellularized lung scaffold and hydrogel on DE formation in comparison with fibronectin-coated cultures, hESC-derived endodermal cells were replated on three different beds (Fig. 2A). At day 15 of lung progenitor differentiation, we observed morphological heterogeneity in fibronectin- (Fig. S2A) and hydrogel- (Fig. S2B) coated cultures. Analysis of H&E-stained cells that have been differentiated on scaffold revealed a subset of epithelial cells that lined the lumen (Fig. S2C) in addition to other cells that were not associated with such anatomical regions. At day 15 of differentiation, cells stained positively for NKX2.1, P63 and FOXA2 (Fig. S2D-E). The majority of cells were positive for these markers in fibronectin-coated cultures (Fig. S2D); while P63 expressing cells were not detected in hydrogel group (Fig. S2E).

The morphology of lung progenitor cells on fibronectin- and hydrogel-coated plates at day 25 is shown in Fig. 3A, B. H&E staining of cells differentiated on scaffold revealed that such cells were located in alveolar structures, particularly in thin alveolar walls. In line with these findings, SEM micrographs showed that the ECM surface was densely covered by differentiated cells (Fig. 3B). Additional immunostaining revealed that cells expressed NKX2.1 at day 25 in both culture conditions and also expressed pro-surfactant protein C (pro-SFTPC), a marker of type 2 alveolar epithelial cells (AT2) (Fig. 3C, D). Differentiated cells on scaffold were analyzed for the expression of (proximal) airway and (distal) AT2

markers at day 25. CK5 and P63 (markers of basal cells) were detected in cells lining the airways while SFTPC and AQP3 (AT2 markers) were observed in alveolar regions (Fig. 3E).

Moreover, gene expression analysis revealed significant upregulation of the DE marker *FOXA2* in cells cultured on fibronectin ($P < 0.0001$) compared with other groups at days 15 and 25 of differentiation. On the other hand, cells differentiated on hydrogel showed significant upregulation in *FOXA2* gene ($P < 0.01$) in comparison with differentiated cells on scaffold at day 25 (Fig. 4). Expression of *SOX9* as distinct marker in distal airways and developing alveolar region showed a significant increase in hydrogel and lung scaffold groups at day 25 ($P < 0.01$ and $P < 0.05$). Interestingly, cells seeded on scaffold showed significant upregulation of *SFTPC* expression ($P < 0.0001$). Finally, markers of differentiated airway epithelium including *FOXJ1* (ciliated cells) and *MUC5A* (secretory cells) showed clear upregulation in cells differentiated using dECM approach at day 25 ($P < 0.001$and $P < 0.0001$, respectively). In addition, expression levels of basal cell markers including *CK5* and *P63* were significantly upregulated in dECM at day 25 ($P < 0.0001$).

4. Discussion

The current study examined the impact of decellularized sheep lung slices (scaffold) and hydrogels on lung progenitor cell differentiation from hESCs. Because of the complex interactions between cells and matrices during lung development, in vitro differentiation of PSC into functional airway and alveolar epithelial cells is a current challenge. Here we report that hESCs can be differentiated toward lung progenitor cells on decellularized lung-derived scaffolds and that the presence of exogenous growth factors phenotypically improves maturation of the cellular descendants in vitro. Another interesting finding is that the native lung ECM structure enhances in vitro AT2 differentiation and subsequently induces *AQP3* and *SFTPC* expression. We also report the emergence of cells expressing markers that are characteristic of distal airway stem/progenitor cells.

Up to now, different approaches were applied to enhance the generation of mature and functional AT2 using various cocktails of exogenous growth factors in an attempt to mimic the native lung niche. Accordingly, patterning of developing proximal airways using acellular lung tissues and differentiation of PSCs into mature airway epithelial cells including ciliated cells, club cells and basal cells have been reported to morphologically and functionally resemble the native airways [17]. It has been shown that matrix topography, being a physical characteristic of the ECM, regulates stem cell differentiation through changing cell shape through a contact guidance process [18]. In 3D structures of normal tissues, ECM fibers (collagen) and their arrangement parallel to the epithelium influence cellular proliferation and differentiation particularly during development [19]. Such mechanotransductive mechanism is therefore involved in the transformation of matrix topographic cues into intracellular signals. The ECM-integrin-cytoskeleton axis is central to this mechanism. The topographic features of the ECM may induce focal adhesion formation triggering intracellular signal transduction [20], which induces nuclear architecture deformation and alteration of gene expression profiles [21].

In this study, we showed that differentiation of human ESC into AT2 using decellularized lung scaffolds led to the generation of cells that were phenotypically characterized by pro-SFTPC and AQP3 expression. Our immunostaining revealed that PSC-derived pro-SFTPC-expressing cells were able to repopulate decellularized alveolar structures in [9]. Repopulation of the scaffold by PSC-derived cells highlights the importance of 3D ECM topographic characteristics in supporting cell adherence and maturation [17]. According to our gene expression analysis, decellularized sheep lung scaffolds successfully induced the differentiation of AFE to heterogeneous populations including bronchiolar airway phenotypes as basal cells (CK5 and P63), ciliated cells (FOXJ1) and secretory cells (MUC5A) markers, as well as distal or peripheral progenitors (NKX2.1 and SOX9) and AT2s (SFTPC) on day 25 [22]. Moreover, our data suggest that PSC-derived progenitors at day 15 may possess bi-potent differentiation capabilities allowing them to give rise to both distal airway and alveolar epithelial cells [23]. After recellularization of lung scaffolds with 15-day-old lung progenitors, bronchiolar airway epithelial cell-associated genes (*FOXJ1* and *MUC5A*) showed a significant upregulation [17].

Natural hydrogels have been extensively generated from various decellularized tissues [24–26] as well as lung-derived tissues [27]. Detergent-based decellularization and enzymatic solubilization of lung tissue methods have been widely used for lung ECM hydrogel preparation [26,28]. In contrast to decellularized lung scaffolds as a 3D culture system, 2D monolayer cultures have been used to induce the transition from PSCs into pro-SFTPC-expressing cells via differentiation on hydrogel. Such method led to the production of typical epithelial cell colonies in 2D cultures. Based on *SFTPC* expression, differentiated cells on fibronectin- and hydrogel-coated plates did not show significant differences in AT2 differentiation. Results derived from the monolayer culture using hydrogel coating were not convincing compared to the 3D culture method; this finding suggests that hydrogel can be used as a surrogate for fibronectin. Although ECM-derived hydrogels preserve the stiffness and viscoelasticity of the intact lung, monolayer cultures using hydrogel do not resemble the lung microenvironment nor mimic native ECM features [29]. In addition, the procedure used to prepare ECM-derived hydrogels have drawbacks including disruption of proteoglycans and ECM-bound growth factors that are need for proper cell behaviors [30,31].

To overcome donor shortage and explore potential therapeutic options for organ failure, xenogeneic organ-derived scaffolds have been recellularized with human cell populations and re-implanted into animal recipients [32]. For example, decellularized porcine lung scaffolds were repopulated by human cells; vascular network and airways were repopulated by human umbilical vein endothelial cells and basal cells, respectively. Vascular reperfusion and gas exchange were achieved after implantation [33]. The limited function of the graft and immune system responses to xenogeneic scaffolds represent serious challenges. However, these challenges may be at least partially overcome by extensive preclinical studies using large animal models to achieve a valid clinical-grade procedure for translating the technology into a robust therapy.

In conclusion, our results revealed improved differentiation of AT2 when cultured on sheep lung-derived scaffolds in comparison with lung ECM-derived hydrogel and fibronectin. We found that the 3D culture of

PSC-derived lung progenitors on lung ECM resulted in strong upregulation of AT2 markers, in addition to efficient cell adherence, maturation and retention in the alveolar region.

Declarations

Acknowledgments:

We gratefully acknowledge Tissue and Cell Engineering Department of Royan institute for their entire valuable support.

Funding:

This research was funded by grants from University of Tehran and Royan Institute (Lotos charity grant). EEA acknowledges the support of the ILH, German Research Foundation (DFG; EL 931/4-1, KFO309 P7 and SFB CRC1213- project A04), University Hospital Giessen and Marburg (UKGM), German Center for Lung Research (DZL) and the Cardio-Pulmonary Institute (CPI, EXC 2026, Project ID: 390649896).

Conflicts of Interest:

The authors declare that there is no conflict of interest.

Authors contribution:

M.R.M.D., S.S.Ch., Y.T., and S.R. designed the study and the experiments, A.N., and Z.Gh. performed the experiments, A.N., F.G. and Z.Gh. analyzed the data, S.S.Ch., A.N., F.G., and S.R. interpreted the results, M.R.M.D., S.S.Ch., Y.T, and H.B. contributed reagents/materials/tools, A.N. and F.G. wrote the manuscript, A.N., F.G. Y.T. and Z.Gh. prepared the illustrations, Y.T, E.E.A. and S.S.Ch. corrected the manuscript and approved its final version.

Data Availibility:

All data generated or analyzed in this study are included in this article and supplementary files.

References

1. Ohata, K. & Ott, H. C. Human-scale lung regeneration based on decellularized matrix scaffolds as a biologic platform. *Surg Today* **50**, 633-643, doi:10.1007/s00595-020-02000-y (2020).
2. Burgstaller, G. *et al.* The instructive extracellular matrix of the lung: basic composition and alterations in chronic lung disease. *Eur Respir J* **50**, doi:10.1183/13993003.01805-2016 (2017).
3. Guilak, F. *et al.* Control of stem cell fate by physical interactions with the extracellular matrix. *Cell Stem Cell* **5**, 17-26, doi:10.1016/j.stem.2009.06.016 (2009).
4. Ashtiani, M. K. *et al.* Substrate-mediated commitment of human embryonic stem cells for hepatic differentiation. *J Biomed Mater Res A* **104**, 2861-2872, doi:10.1002/jbm.a.35830 (2016).

5. Ullah, I. *et al.* Adult Tissue Extracellular Matrix Determines Tissue Specification of Human iPSC-Derived Embryonic Stage Mesodermal Precursor Cells. *Adv Sci (Weinh)* **7**, 1901198, doi:10.1002/advs.201901198 (2020).
6. Bonnans, C., Chou, J. & Werb, Z. Remodelling the extracellular matrix in development and disease. *Nat Rev Mol Cell Biol* **15**, 786-801, doi:10.1038/nrm3904 (2014).
7. Takasato, M. & Little, M. H. Making a Kidney Organoid Using the Directed Differentiation of Human Pluripotent Stem Cells. *Methods Mol Biol* **1597**, 195-206, doi:10.1007/978-1-4939-6949-4_14 (2017).
8. Gilpin, S. E. *et al.* Enhanced lung epithelial specification of human induced pluripotent stem cells on decellularized lung matrix. *Ann Thorac Surg* **98**, 1721-1729; discussion 1729, doi:10.1016/j.athoracsur.2014.05.080 (2014).
9. Ghaedi, M. *et al.* Human iPS cell-derived alveolar epithelium repopulates lung extracellular matrix. *J Clin Invest* **123**, 4950-4962, doi:10.1172/JCI68793 (2013).
10. Mitchell, A., Drinnan, C. T., Jensen, T. & Finck, C. Production of high purity alveolar-like cells from iPSCs through depletion of uncommitted cells after AFE induction. *Differentiation* **96**, 62-69, doi:10.1016/j.diff.2017.08.001 (2017).
11. Jacob, A. *et al.* Differentiation of Human Pluripotent Stem Cells into Functional Lung Alveolar Epithelial Cells. *Cell Stem Cell* **21**, 472-488 e410, doi:10.1016/j.stem.2017.08.014 (2017).
12. van Riet, S. *et al.* In vitro modelling of alveolar repair at the air-liquid interface using alveolar epithelial cells derived from human induced pluripotent stem cells. *Sci Rep* **10**, 5499, doi:10.1038/s41598-020-62226-1 (2020).
13. Cornwell, K. G., Landsman, A. & James, K. S. Extracellular matrix biomaterials for soft tissue repair. *Clin Podiatr Med Surg* **26**, 507-523, doi:10.1016/j.cpm.2009.08.001 (2009).
14. Daly, K. A. *et al.* Effect of the alphaGal epitope on the response to small intestinal submucosa extracellular matrix in a nonhuman primate model. *Tissue Eng Part A* **15**, 3877-3888, doi:10.1089/ten.TEA.2009.0089 (2009).
15. Stahl, E. C. *et al.* Evaluation of the host immune response to decellularized lung scaffolds derived from alpha-Gal knockout pigs in a non-human primate model. *Biomaterials* **187**, 93-104, doi:10.1016/j.biomaterials.2018.09.038 (2018).
16. Mokhber Dezfouli, M. R. *et al.* Hydrocortisone Promotes Differentiation of Mouse Embryonic Stem Cell-Derived Definitive Endoderm toward Lung Alveolar Epithelial Cells. *Cell J* **20**, 469-476, doi:10.22074/cellj.2019.5521 (2019).
17. Shojaie, S. *et al.* Acellular lung scaffolds direct differentiation of endoderm to functional airway epithelial cells: requirement of matrix-bound HS proteoglycans. *Stem Cell Reports* **4**, 419-430, doi:10.1016/j.stemcr.2015.01.004 (2015).
18. Clark, P., Connolly, P., Curtis, A. S., Dow, J. A. & Wilkinson, C. D. Topographical control of cell behaviour. I. Simple step cues. *Development* **99**, 439-448 (1987).
19. Provenzano, P. P., Inman, D. R., Eliceiri, K. W., Trier, S. M. & Keely, P. J. Contact guidance mediated three-dimensional cell migration is regulated by Rho/ROCK-dependent matrix reorganization.

Biophys J **95**, 5374-5384, doi:10.1529/biophysj.108.133116 (2008).

20. Bettinger, C. J., Langer, R. & Borenstein, J. T. Engineering substrate topography at the micro- and nanoscale to control cell function. *Angew Chem Int Ed Engl* **48**, 5406-5415, doi:10.1002/anie.200805179 (2009).
21. Dalby, M. J., Riehle, M. O., Yarwood, S. J., Wilkinson, C. D. & Curtis, A. S. Nucleus alignment and cell signaling in fibroblasts: response to a micro-grooved topography. *Exp Cell Res* **284**, 274-282, doi:10.1016/s0014-4827(02)00053-8 (2003).
22. Swarr, D. T., Wert, S. E. & Whitsett, J. A. in *Kendig's Disorders of the Respiratory Tract in Children* 26-39. e24 (Elsevier, 2019).
23. Nikolic, M. Z. *et al.* Human embryonic lung epithelial tips are multipotent progenitors that can be expanded in vitro as long-term self-renewing organoids. *Elife* **6**, doi:10.7554/eLife.26575 (2017).
24. Johnson, T. D. *et al.* Human versus porcine tissue sourcing for an injectable myocardial matrix hydrogel. *Biomater Sci* **2014**, 60283D, doi:10.1039/C3BM60283D (2014).
25. Loneker, A. E., Faulk, D. M., Hussey, G. S., D'Amore, A. & Badylak, S. F. Solubilized liver extracellular matrix maintains primary rat hepatocyte phenotype in-vitro. *J Biomed Mater Res A* **104**, 1846-1847, doi:10.1002/jbm.a.35778 (2016).
26. Saldin, L. T., Cramer, M. C., Velankar, S. S., White, L. J. & Badylak, S. F. Extracellular matrix hydrogels from decellularized tissues: Structure and function. *Acta Biomater* **49**, 1-15, doi:10.1016/j.actbio.2016.11.068 (2017).
27. Pouliot, R. A. *et al.* Development and characterization of a naturally derived lung extracellular matrix hydrogel. *J Biomed Mater Res A* **104**, 1922-1935, doi:10.1002/jbm.a.35726 (2016).
28. Choudhury, D., Tun, H. W., Wang, T. & Naing, M. W. Organ-Derived Decellularized Extracellular Matrix: A Game Changer for Bioink Manufacturing? *Trends Biotechnol* **36**, 787-805, doi:10.1016/j.tibtech.2018.03.003 (2018).
29. de Hilster, R. H. J. *et al.* Human lung extracellular matrix hydrogels resemble the stiffness and viscoelasticity of native lung tissue. *Am J Physiol Lung Cell Mol Physiol* **318**, L698-L704, doi:10.1152/ajplung.00451.2019 (2020).
30. Crapo, P. M., Gilbert, T. W. & Badylak, S. F. An overview of tissue and whole organ decellularization processes. *Biomaterials* **32**, 3233-3243, doi:10.1016/j.biomaterials.2011.01.057 (2011).
31. Mendoza-Novelo, B. *et al.* Decellularization of pericardial tissue and its impact on tensile viscoelasticity and glycosaminoglycan content. *Acta Biomater* **7**, 1241-1248, doi:10.1016/j.actbio.2010.11.017 (2011).
32. Zhou, H. *et al.* Bioengineering Human Lung Grafts on Porcine Matrix. *Ann Surg* **267**, 590-598, doi:10.1097/SLA.0000000000002129 (2018).
33. Wiles, K., Fishman, J. M., De Coppi, P. & Birchall, M. A. The Host Immune Response to Tissue-Engineered Organs: Current Problems and Future Directions. *Tissue Eng Part B Rev* **22**, 208-219, doi:10.1089/ten.TEB.2015.0376 (2016).

Figures

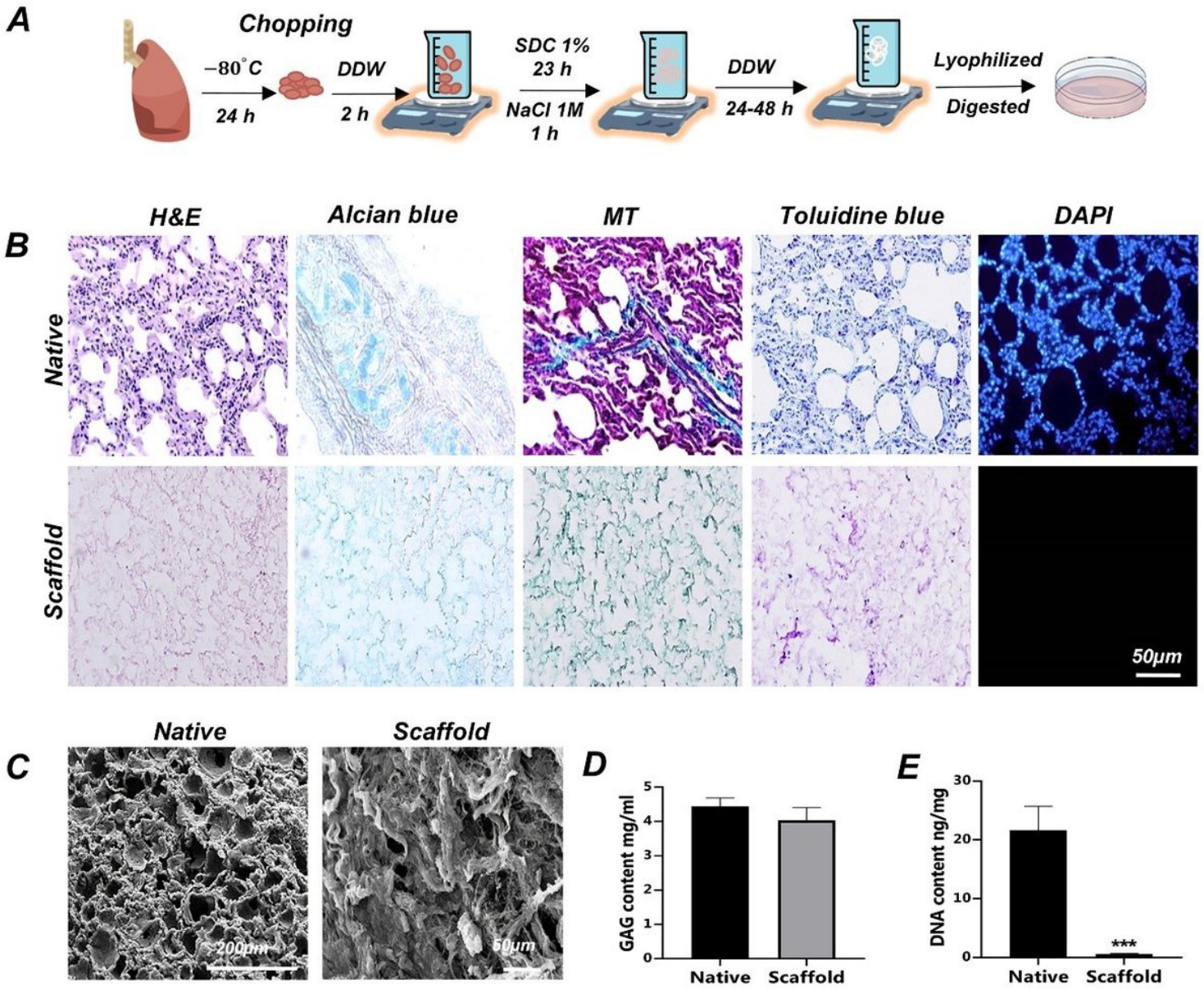

Figure 1

Decellularization protocol, hydrogel formation and characterization. (A) schematic representation of lung decellularization protocol; DDW, double distilled water; SDC, sodium deoxycholate; PBS, Phosphate Buffered Saline (B) Histological analysis of native sheep lung with sheep decellularized lung (dECM) using H&E, Alcian blue, Masson's trichrome (MT), Toluidine blue and DAPI staining (n=3). (C) Representative scanning electron microscopy (SEM) photomicrographs of native lung and lung ECM-derived scaffold. (D) Quantification of GAGs content of native and scaffold indicate high-ly preservation of GAGs after decellularization (n = 4). (E) DNA content assay shows significant re-moval of DNA after the devitalization procedure (n = 3, ***p < .001).

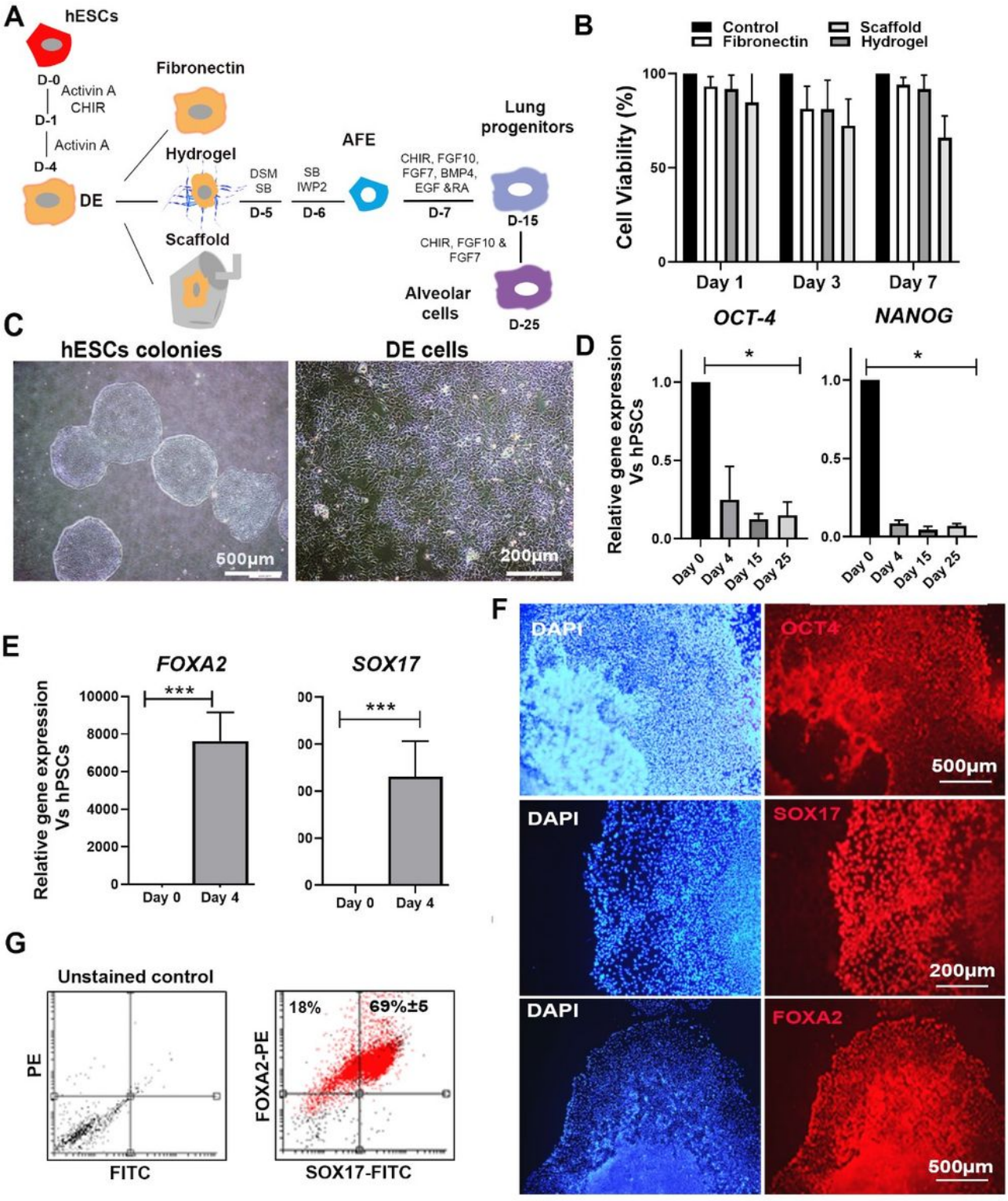

Figure 2

Morphology and phenotypically characterization of hPSC-derived definitive endoderm before re-plating, (A) schematic representation of lung differentiation protocol showing differentiation of Em-bryonic stem cells (ESCs) into endoderm cells in presence of small molecules and growth factors and replating lung progenitors on different beds including fibronectin, hydrogel and scaffold at day 15. (B) determination of cell viability percentage by MTS assay at days 1, 3 and 7 after A549 cell line culture on different beds (n =

4). (C) Phase-contrast images of typical hPSC colonies and definitive endoderm cells. (D) qRT-PCR analysis confirms a significant decrease of hESCs pluripotent genes at days 4,15 and 25 of lung progenitor differentiation. (E) qRT-PCR analysis for FOXA2 and SOX17 genes at day 4 of differentiation compared to hESCs. (F) Immunostaining shows expression of OCT4 in hPSC and expression of FOXA2 and SOX17 markers in endoderm cells. (G) Flow cytometrically analysis of FOXA2 and SOX17 expressing cells (n = 3).

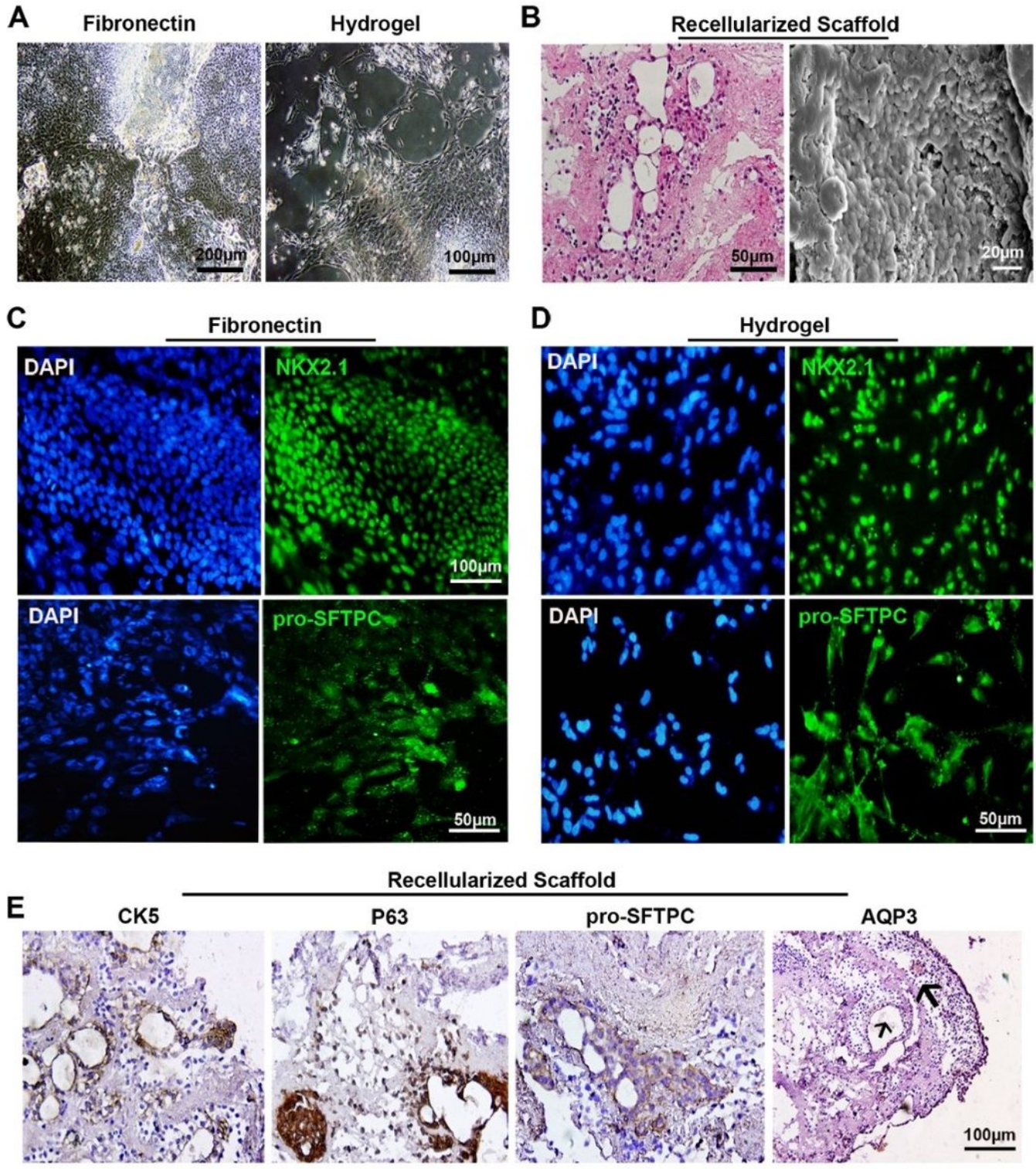

Figure 3

Morphology and phenotypically characterization of hPSC-derived lung progenitor cells at day 25 of differentiation, (A) Phase-contrast images of cells grown on fibronectin and hydrogel at day 25. (B) H&E staining shows the attachment and retention of differentiated cells at day 25 and SEM photomi-crograph shows the recellularization of scaffold surface seeded with 15-day-old progenitor cells after 21 days. (C) Immunostaining for NKX2.1 and PRO-SPC in lung progenitor cells grown on fibronectin and (D) hydrogel at day 25. (E) Immunohistochemistry for pro-SFTPC, AQP3, CK5 and P63 markers in cells grown on scaffold at day 25.

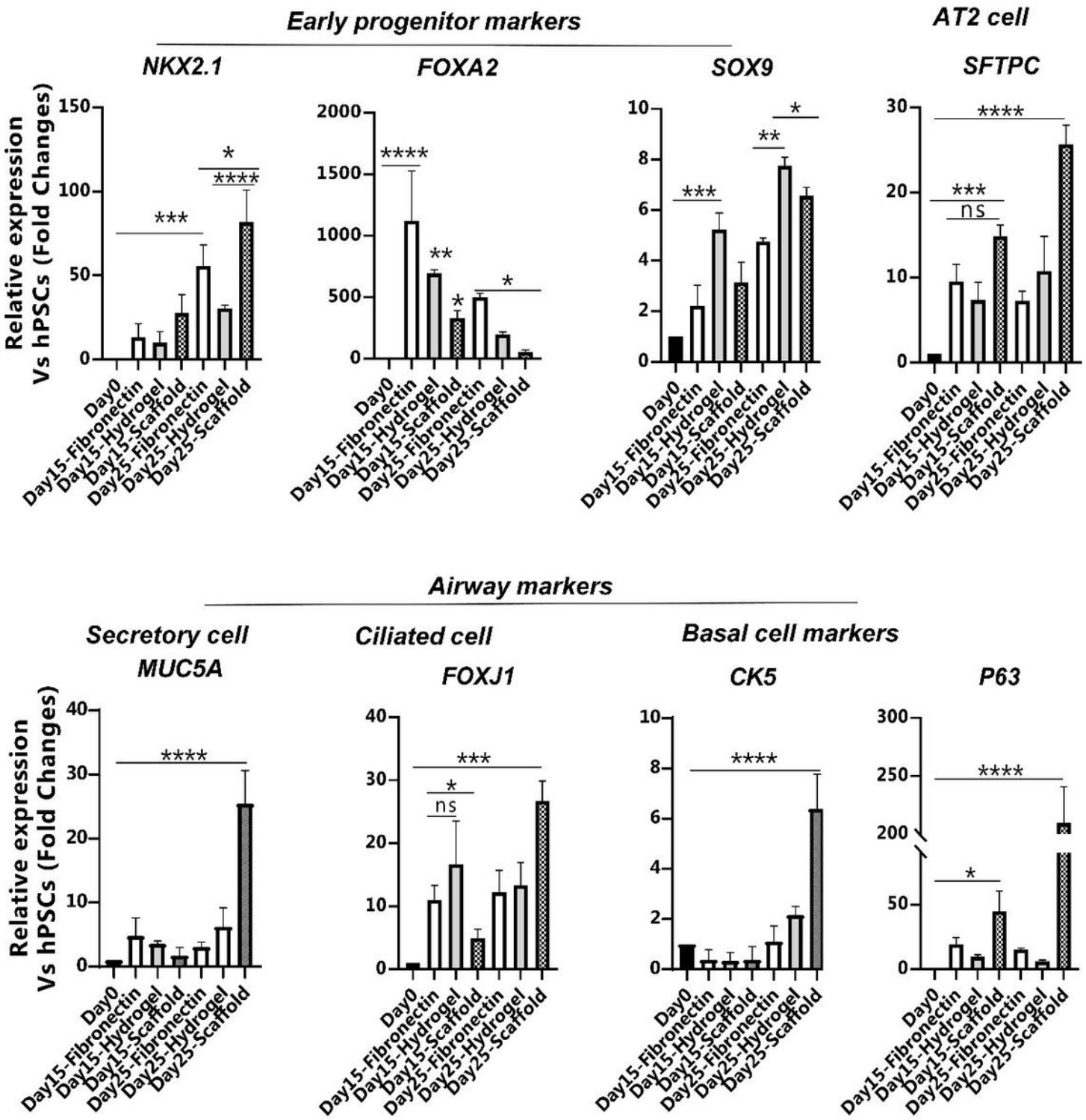

Figure 4

Quantitative RT-PCR analysis of undifferentiated human embryonic stem cells (hESCs) and differen-tiated cells for SOX9, FOXJ1, FOXA2, NKX2.1, MUC5A, P63, SPC and CK5 genes at day 15 and 25 of lung progenitor cells. The expression level of target gene was normalized to GAPDH and presented relative to hESC. Data are presented as mean ± SD. Significant difference was determined by the t-test with unequal variance; ($p<0.05$ *, $p<0.01$**, $p<0.001$*** and $p<0.0001$****), n=3.

Supplementary Files

This is a list of supplementary files associated with this preprint. Click to download.

- Supplementaryfiles.pdf